HHS Public Access

Author manuscript

Circulation. Author manuscript; available in PMC 2017 January 26.

Published in final edited form as:

Circulation. 2016 January 26; 133(4): 409–421. doi:10.1161/CIRCULATIONAHA.115.017537.

Targeting NCK-Mediated Endothelial Cell Front-Rear Polarity Inhibits Neo-Vascularization

Alexandre Dubrac, PhD[1], **Gael Genet, PhD**[1], **Roxana Ola, PhD**[1], **Feng Zhang, PhD**[1], **Laurence Pibouin-Fragner, PhD**[2], **Jinah Han, PhD**[1], **Jiasheng Zhang, MD**[1], **Jean-Léon Thomas, PhD**[1,3,4], **Alain Chedotal, PhD**[5], **Martin A. Schwartz, PhD**[1,6], and **Anne Eichmann, PhD**[1,2,7]

[1]Cardiovascular Research Center, Yale University School of Medicine, New Haven, CT

[2]INSERM U1050, Collège de France, Center for Interdisciplinary Research in Biology (CIRB), Paris, France

[3]Department of Neurology, Yale University School of Medicine, New Haven, CT

[4]Institut du Cerveau et de la Moelle, Inserm, Université Pierre et Marie Curie, Paris, France

[5]Sorbonne Universités, UPMC Universités Paris 06, INSERM, UMR_S968, CNRS, UMR_7210, Institut de la Vision, Paris, France

[6]Departments of Cell Biology and Biomedical Engineering, Yale University, New Haven, CT

[7]Department of Cellular and Molecular Physiology, Yale University School of Medicine, New Haven, CT

Abstract

Background—Sprouting angiogenesis is a key process driving blood vessel growth in ischemic tissues and an important drug target in a number of diseases, including wet macular degeneration and wound healing. Endothelial cells forming the sprout must develop front-rear polarity to allow sprout extension. The adaptor proteins Nck1 and 2 are known regulators of cytoskeletal dynamics and polarity, but their function in angiogenesis is poorly understood. Here we show that the Nck adaptors are required for endothelial cell front-rear polarity and migration downstream of the angiogenic growth factors VEGF-A and Slit2.

Methods and Results—Mice carrying inducible, endothelial-specific *Nck1/2* deletions fail to develop front-rear polarized vessel sprouts and exhibit severe angiogenesis defects in the postnatal retina and during embryonic development. Inactivation of *NCK1* and *2* inhibits polarity by preventing Cdc42 and Pak2 activation by VEGF-A and Slit2. Mechanistically, NCK binding to ROBO1 is required for both Slit2 and VEGF induced front-rear polarity. Selective inhibition of polarized endothelial cell migration by targeting *Nck1/2* prevents hypersprouting induced by

Correspondence: Anne Eichmann, PhD, Yale University School of Medicine, Section of Cardiovascular Medicine, Department of Internal Medicine, 300 George St., 7th floor, New Haven, CT 06511, Phone: 203-737-5205, Fax: 203-785-7144, anne.eichmann@yale.edu.

Disclosures: None.

Notch or Bmp signaling inhibition, as well as pathological ocular neovascularization and wound healing.

Conclusions—These data reveal a novel signal integration mechanism involving NCK1/2, ROBO1/2 and VEGFR2 that controls endothelial cell front-rear polarity during sprouting angiogenesis.

Keywords

Angiogenesis; Polarity; Migration; Slit-Robo; Guidance; Vascular biology

Introduction

Sprouting angiogenesis is a morphogenetic process that is critical in embryonic development and adult pathologies including wet age-related macular degeneration (AMD), wound healing, cancer and rheumatoid arthritis[1–4]. Angiogenesis is usually induced by production of VEGF in tissues subject to hypoxia or other insults. The resultant VEGF gradients stimulate endothelial cells through VEGF receptor 2 (VEGFR2) to induce sprout formation, a highly dynamic process that entails collective migration toward the VEGF source, with endothelial cells polarizing and migrating in an ordered fashion. Sprouting is followed by formation of endothelial tubes, initiation of blood flow and vessel stabilization[1–4].

VEGF is critical for endothelial cell migration, proliferation and survival, and has consequently been a major target for anti-angiogenic therapy, although its use is limited by side effects including hypertension, proteinuria and thrombosis[3–5]. However, like all complex morphogenetic processes, angiogenesis depends on many other microenvironmental influences, including extracellular matrix, cell-cell interactions and other soluble factors[6, 7]. Identifying these factors and elucidating the mechanisms by which cells integrate information from multiple stimuli is a major challenge. This information will also be essential for the development of more effective and specific therapeutics.

Endothelial cell polarity is a key feature of angiogenic sprouting. Tip cells leading the sprout extremity reorganize their cytoskeleton to establish front-rear polarity by extending lamellipodia and filopodia at the leading front. The rear end of the tip cell remains attached through cell-cell junctions to other endothelial cells termed stalk cells that adopt apico-basal polarity and establish a lumen. Thus, sprouting entails a switch from apico-basal to front-rear polarity. Front-rear polarity requires proper orientation of the Golgi apparatus and the microtubule-organizing center towards the leading edge. Evidence in other cell types suggests that establishment of front-rear polarity requires signaling through the small GTPase Cdc42[8–10]. However, Cdc42 and Rac1 also regulate filopodia and lamellipodia formation at the leading edge, and establishment of apico-basal polarity[11]. The molecular mechanisms regulating and coordinating decisions to establish front-rear and apico-basal polarity are poorly understood.

Here, we report that Nck adaptor proteins are selectively required for establishment of front-rear polarity in sprouting endothelial cells. Nck is evolutionarily conserved and has one homologue in Drosophila (Dock) and two members in mice and humans (Nck-1 and

Nck-2)[12–14]. The two murine Nck proteins have broad and overlapping expression patterns and function redundantly, as deletion of each individual *Nck* gene is compatible with life, while combined knockout leads to gastrulation defects and embryonic lethality at E9.5[14]. The biological function of Nck/Dock is to link cell surface receptors to the actin cytoskeleton. Nck-1 shows ~68% amino acid identity to Nck-2 and their SH2 domain binds a common set of phosphopeptides with equivalent binding affinity[12, 13]. Their three N-terminal SH3 domains interact with PAK1-3 and their upstream activators, Rac1/Cdc42. Activated PAK then regulates cytoskeletal dynamics.

In endothelial cells, NCKs bind to phosphorylated Tyr1214 of VEGFR2 allowing activation of PAK, Cdc42 and migration in vitro[15]. Nck also binds the Robo1 and 2 receptors for Slits, secreted guidance molecules[16, 17]. Rac1 activation downstream of Slit-Robo signaling requires the binding of Nck to a proline-rich region (PRR) in the intracellular part of Robo[16–18]. We recently showed that Slit2-Robo1/2 signaling is essential for retinal angiogenesis and that ROBO1 and 2 are selectively required for RAC1 and PAK2 activation in response to Slit2 and VEGF-A[19]. Here we show that Nck1/2 are an essential component of the VEGF-A and Slit2 signaling machinery driving tip cell front-rear polarity and migration *in vivo* and that selectively targeting endothelial cell polarity dramatically inhibits developmental and pathological neovascularization.

Materials and Methods

A detailed Methods section is provided in the Supplement Material.

Mice

Mice were maintained in the Animal Research Center and experiments were performed under a protocol approved by the Institutional Animal Care and Use Committee of Yale University. Gene deletion was induced by intraperitoneal injections with 50μg tamoxifen (Sigma, T5648; 1 mg/ml) to pups at P1, P2, P3 and mice were sacrificed at P5. To observe the vascular deeper layer formation 100μg tamoxifen was injected at P5 and P6 and mice were sacrificed at P12. For the wound healing experiment, 6 weeks old mice were injected with 2mg of tamoxifen five times every alternate day.

For rescue experiments, pups were injected once a day with DAPT (P4, 100mg/kg) or Bmp9 and 10 blocking antibodies (P4, 10mg/kg). Control pups were injected once a day with the same amount of vehicle or control antibody.

Adenoviral constructs

Adenoviral Robo1-FC was obtained by PCR amplification of the rat Robo1 extracellular domain (aa31-aa258) that was fused to Fc by insertion into pFUSE-hIgG1-Fc1 (InvivoGen) and then subcloned into pENTR1A (Invitrogen). Thereafter, inserts were transferred into pAd/CMV/V5/DEST using the Gateway System (Invitrogen). Adenoviruses expressing GFP-tagged Robo1 full length (Robo1WT, amino acids 27-1651), Robo1ΔPRR (deletion between amino acids 1,208–1,487) or Robo1ΔCD (amino acids 1-948) were generated by PCR from rat cDNA and fused to IgK signal peptide (METDTLLLWVLLLWVPGSTGD). To make adenovirus, HEK293 cells were transfected and the adenovirus containing

supernatant was harvested and purified with the Adeno-X Maxi Purification Kit (Clontech). The titer of the virus was determined using Adeno-X Rapid Titer Kit (Clontech) according to the manufacturer's instructions. Mouse pups were injected intraperitoneally with 5×10^8 pfu/30 to 50 μl at day 0, 1, 2, 3 and 4 and sacrificed at P5.

Scratch assay and analysis of cell polarity

Confluent HUVEC monolayers were grown in 6-well plates. 24h after siRNA transfection, the cells were starved 18 hours in EBM-2 medium with 1% FBS. A horizontal wound was created using a sterile 200μl pipette tip. Next, the cells were washed with EBM2 at 37°C and incubated in EBM-2 supplemented with VEGF-A (25 ng/ml) or Slit2 (1 μg/ml) at 37°C for 16 hours. Pictures of scratch wounds were taken just before stimulation (time 0) and after 16h. Migration was calculated using ImageJ software.

For the polarity assay, the confluent monolayers of HUVECs were grown on gelatin-coated coverslips, starved 18 hours and incubated in EBM-2 supplemented with VEGF-A (25 ng/ml) or Slit2 (1 μg/ml) at 37°C in CO2 incubator for 2 hours.

Subsequently, cells were fixed in 4% paraformaldehyde in PBS for 10 minutes and permeabilized in 0.1% Triton X-100 in PBS for 10 minutes. After blocking, cells were incubated overnight in primary antibody at 4°C (GM130, 1:500 in 1% BSA in PBS). Cells were then incubated with the secondary antibody, DAPI and CY3-phalloidin for 1h at room temperature. Images were captured using with a Perkin Elmer UltraVIEW VoX spinning disc confocal microscope equipped with a 20X dry objective and a 63X oil immersion lens. The polarity was determined for the cells at the wound edge. The cells with the Golgi localized within the 120° angle in front of the nucleus facing the axis of the wound, were quantified as polarized. A total of 120–150 cells from each of four independent experiments were analyzed to determine the polarity index.

Statistical analysis

All data are shown as mean ± standard error of the mean (SEM). Statistical analyses were performed for all quantitative data using Prism 6.0 (Graph Pad).

RESULTS

Nck1 and 2 modulate sprouting angiogenesis

We determined if *Nck* is required for vascular development, focusing first on the postnatal mouse retina, which is a useful model to study angiogenesis[20]. Since mouse endothelial cells express Nck1 and 2[21], we generated inducible, endothelial specific *Nck2* deletions using *Nck2*^{lox} mice[22, 23] and the *Cdh5Cre*^{ERT2} line[24] (hereafter referred to as *Nck2iec*) in *Nck1*$^{-/-}$ *mice*. Tamoxifen (Tx) was injected at birth (P1/2/3) and retinas were analyzed at P5. We confirmed the efficiency of *Nck* deletion in tamoxifen-injected mice by Western-blot and qPCR (Figure 1A, Supplementary Figure 1A–B). Isolectin B4 (IB4) staining of the retinal vasculature showed that angiogenesis was severely impaired in *Nck1*$^{-/-}$*Nck2iec* double mutant mice (Figure 1B–C, Supplementary Figure 1C–D). *Nck1*$^{-/-}$ single knockout littermates showed no vascular defects, while *Nck2iec* single mutants exhibited mild

angiogenesis defects that were further aggravated by deletion of one allele of *Nck1*, and combined deletion of both *Nck* genes led to severely reduced vessel density, branching and vascular radial expansion (Figure 1B–C, Supplementary Figure 1D). *Nck1*$^{-/-}$*Nck2iec* also showed impaired formation of the deeper vascular retinal layers at P12 when gene deletion was initiated at P6 (Figure 1D). Finally, combined deletion of both *Nck* genes also impaired embryonic angiogenesis and sprouting of vessels into the brain at E11 following Tx administration at E9.5 (Figure1E, Supplementary Figure1E–F). Together, these data show that Nck1 and 2 are required for normal embryonic and postnatal sprouting angiogenesis *in vivo*.

Nck1 and 2 regulate tip cell front-rear polarity

The number of angiogenic sprouts at the vascular front of *Nck1*$^{-/-}$*Nck2iec* retinas was decreased when compared with *Nck1*$^{-/-}$ single mutants or wildtype littermates, although tip cell filopodia formation occurred normally (Figure 2A, B). To determine the cause of impaired sprouting in *Nck1*$^{-/-}$*Nck2iec* mice, we counted endothelial cell numbers by labeling with anti-Erg1/2/3 transcription factors[25], which revealed lower overall numbers in *Nck1*$^{-/-}$*Nck2iec* than in *Nck1*$^{-/-}$ mice, although cell number normalized to the vessel area was similar between genotypes (Supplementary Figure 2A–B). Edu injection 4h prior to sacrifice showed decreased numbers of Edu+/IB4+ endothelial cells in *Nck1*$^{-/-}$*Nck2iec* compared to *Nck1*$^{-/-}$ retinas (Supplementary Figure 2C–D), indicating that impaired proliferation contributes to the decreased vessel density in Nck mutants. However, *NCK1* and *2* knockdown in human umbilical vein endothelial cells (HUVECs) failed to affect growth factor-induced proliferation, as shown previously[21] (Supplementary Figure 2E–G). We found no difference in caspase-3+ apoptotic cells and analysis of Collagen IV-positive, IB4 negative empty basement membrane sleeves showed no difference in vessel regression between genotypes (Supplementary Figure 3A–C). Thus, lack of Nck does not impair vascular development by affecting endothelial cell death or vessel stability. *Nck1*$^{-/-}$*Nck2iec* retinas also showed no defect in pericyte or smooth muscle cell recruitment (Supplementary Figure 3D–E).

Tip cells exhibit high levels of Vegf signaling, while adjacent stalk cells show high Notch and Alk1 signaling[26, 27]. To determine if abnormal sprout morphology in *Nck1*$^{-/-}$*Nck2iec* was due to altered Vegf, Notch or Alk signaling, we stained for the Notch ligand Dll4 in retinal wholemounts. Dll4 expression was similar in *Nck1/2* double knockouts compared to single *Nck1* mutant littermates (Supplementary Figure 4A). Likewise, in HUVECs transduced with *NCK1* and *2* siRNA, VEGF-induced mRNA levels of *DLL4* and other tip cell marker genes including *ANG2* and *ESM1*[28] were not significantly altered. *NCK1* and *2* knockdown also did not affect the expression levels of the ALK downstream target *ID1* or of *VEGFR2* and *NRP1* (Supplementary Figure 4B). Thus, altered morphology of sprouting vessels at the vascular front in *Nck1*$^{-/-}$*Nckiec* mice occurs despite normal expression of Vegf, Notch and Alk signaling components.

We then considered that alterations of cell movement might contribute to the observed defects. Cell polarity is a key component of angiogenic migration, thus we analyzed front-rear and apico-basal polarity by staining with IB4, ERG1/2/3 and an anti-GM130 antibody

to label the Golgi apparatus. While 40% of control tip cells had their Golgi positioned towards the leading edge in front of the nucleus, 40% of *Nck1*$^{-/-}$*Nck2iec* tip cells had their Golgi positioned behind the nucleus away from the leading edge (Figure 2C), demonstrating impaired front-rear polarization in *Nck1*$^{-/-}$*Nck2iec* tip cells. Apico-basal polarity of endothelial cells in the stalk position and in the remodeling plexus appeared normal, as shown by Podocalyxin (Pdx) staining of the luminal endothelial cell membrane (Figure 2D, Supplementary Figure 4C). VE-cadherin, which is important for lumen formation *in vivo* [29–31] also showed no difference between genotypes (Supplementary Figure 4D). Nck1 and 2 therefore modulate vascular development by regulating front-rear polarization of sprouting tip cells.

VEGF-A and Slit2 induce endothelial front-rear polarity via NCK1 and 2

NCK is an adapter protein that can potentially coordinate the activities of multiple signaling components. In addition to mediating VEGF-A induced activation of PAK2, CDC42 and RAC1 in vitro[15], NCK functions downstream of ROBO1 in drosophila axons and kidney podocytes[16–18], and we recently showed that Slit2/ROBO1-2 signaling controls endothelial cell migration[19]. We therefore tested effects of NCK1 and 2 in response to VEGF and Slit2 (Figure 3A). Co-immunoprecipitation showed that NCK constitutively associated with ROBO1 in HUVECs, and associated with VEGFR2 after stimulation with Slit2 or VEGF (Figure 3B). Functionally, combined *NCK1/2* siRNA abolished VEGF-A and Slit2 induced HUVEC sprouting in 3D fibrin gels and endothelial cell migration in scratch wound assays (Figure 3C–F). Imaging of cells at the wound edge showed that combined *NCK1/2* siRNA suppressed VEGF-A and Slit2 induced lamellipodia and inhibited polarization of the Golgi apparatus towards the leading edge (Figure 3G–H, Supplementary Figure 5). *NCK1 and 2* siRNA abolished CDC42 and PAK activation in response to VEGF-A and Slit2 (Figure 3I–L). Likewise, endothelial cells isolated from *Nck1*$^{-/-}$*Nck2iec* mice failed to activate PAK in response to VEGF (Figure 3M–N), whereas absence of *Nck1* or *2* alone led to normal Pak activation and cell migration (Figure 3M–N, Supplementary Figure 6A, D–E). Combined *NCK 1* and *2* deletions in mouse or human endothelial cells also reduced VEGFR2 Y1212/4 phosphorylation following VEGF-A treatment (Supplementary Figure 6B–G), but did not affect activation of VEGFR2 Y1173/5 and downstream ERK phosphorylation (Supplementary Figure 6B–G). These data show that NCK1 and 2 are required for formation of a leading edge and establishment of front-rear cell polarity in response to VEGF-A and Slit2 in vitro.

NCK interacts with ROBO1 and VEGFR2 to drive polarity

We had previously shown that Robo1 and 2 are essential for Vegf-a induced Rac activation[19], suggesting that Robos could also be important for Vegf-a induced polarity. Indeed, *ROBO1/2* siRNA abolished Golgi polarization and CDC42 activation in response to VEGF-A and Slit2 (Supplementary Figure 7A–B). To test the role of Slit2 in polarized tip cell migration *in vivo*, we treated neonatal mice with adenovirus encoding Robo1-Fc, which sequesters Slit2[19, 32]. Robo1-Fc adenovirus resulted in a highly significant decrease in Golgi orientation towards the front compared to control virus (Figure 4A–B), indicating that Robo1 signaling cooperates with Vegf-a to establish front-rear cell polarity in retinal tip cells.

These results suggested that NCK could link ROBO1 and VEGFR2 signaling. If so, inhibiting NCK binding to ROBO1 is expected to affect both Slit2 and VEGF signaling. We first tested if inhibition of Slit2/ROBO signaling affected NCK interaction with VEGFR2. *ROBO1/2* siRNA inhibited VEGF-induced co-IP between NCK1 and VEGFR2 (Figure 4C), suggesting that ROBO1/2 enhances VEGF-induced NCK interaction with VEGFR2.

Next, we reconstituted *ROBO1/2* knockdown HUVECs with adenoviral vectors encoding siRNA resistant rat full-length Robo1 (Robo1WT) or truncated versions lacking the proline-rich domain (Robo1ΔPRR) that binds NCK[18]. We also used a control construct lacking the entire Robo1 cytoplasmic domain (Robo1ΔCD), and tagged all constructs with GFP to visualize their expression (Figure 4D). Adenoviral titers were adjusted to re-express near-physiological levels of the rescue constructs, as determined by Western blotting with an anti-Robo1 antibody (Figure 4E). Immunoprecipitation with GFP followed by immunoblotting with NCK antibodies showed that NCK binding was strongly impaired in cells expressing Robo1ΔPRR and lost in cells expressing Robo1ΔCD (Figure 4F), indicating that the proline-rich repeat indeed contains residues critical for NCK binding to Robo1. We next performed scratch wound assays with reconstituted cells and tested front-rear polarity in response to VEGF and Slit2. Expression of Ad-Robo1WT in *ROBO1/2* knockdown cells fully rescued front-rear polarity in response to both VEGF and Slit2, while neither Robo1ΔPRR nor Robo1ΔCD rescued polarity in response to either factor (Figure 4G–H). Furthermore, PAK activation in response to VEGF was rescued by Robo1WT, but not by Robo1ΔPRR or Robo1ΔCD (Figure 4I–J).

Because Nck1 and 2 deletions affected Vegfr2 phosphorylation (Supplementary Figure 6D–G), we next examined if Slit2/ROBO1 signaling regulates VEGFR2 Y1214 phosphorylation in HUVECs as well. In contrast to VEGF-A, Slit2 treatment alone did not induce any VEGFR2 phosphorylation, but combined VEGF-A and Slit2 stimulation enhanced Y1214 phosphorylation (Supplementary Figure 7C). Moreover, Y1214 phosphorylation was blocked by *ROBO1/2* knockdown while Y1175 was again unaffected (Supplementary Figure 7D), leading to a global VEGFR2 phosphorylation reduction, as determined by VEGFR2 immunoprecipitation followed by western blot for phosphotyrosine (Supplementary Figure 7E). Thus, SLIT2-ROBO1/2 signaling cooperates with VEGF-A in activation of Y1214.

These data show that NCK binding to the ROBO1 cytoplasmic domain is required for VEGF-induced NCK interaction with VEGFR2, downstream PAK activation and establishment of front-rear polarity in vitro.

Polarity defects prevent hyper-sprouting induced by Notch1 and Alk1 inhibition

Blocking Notch1 potently induces a hyper-sprouting phenotype in the retina[2, 33, 26] (Figure 5A), prompting us to test if pharmacological Notch inhibition could rescue sprouting in *Nck1*$^{-/-}$*Nck2iec* mice. The gamma secretase inhibitor DAPT induced significant hyper-sprouting in *Nck1*$^{-/-}$ mice, while its effect was strongly inhibited in the *Nck1*$^{-/-}$*Nck2iec* retina (Figure 5A). Blocking the bone morphogenetic protein (BMP) 9/10 receptor Alk1 also leads to retinal hypervascularization[27, 34, 35] (Figure 5B). However, deletion of Nck1/2 also failed to induce hyper-sprouting after BMP9/10 blockade (Figure 5B). Nck1 and 2 mediated front-rear polarity is therefore required for hyper-sprouting induced by both Notch1 and

Alk1 inhibition. These results stress the crucial function of Nck mediated front-rear polarity in the tip cell during neovascularization.

Blocking Nck1 and 2 inhibits pathological angiogenesis

To determine the relevance of Nck mediated front-rear polarity in pathological neovascularization, we subjected *Nck1*$^{-/-}$*Nck2iec* mice to oxygen-induced retinopathy, which leads to pathological sprouting and formation of abnormal vascular tufts that are leaky and prone to bleeding, mimicking vision-threatening defects seen in AMD patients. Induction of *Nck2* deletion was done after exposure to hyperoxia, during the neovascularization period (p12-p17) (Figure 6A). Vaso-obliteration at this stage was comparable between *Nck1*$^{-/-}$*Nck2iec* mice and littermate controls (Supplementary Figure 8A). Both *Nck1*$^{-/-}$*Nck2iec* mice showed reduced hemorrhage and severely reduced angiogenesis and vascular tuft formation (Figure 6B–D, Supplementary Figure 8B, C). Thus, blockade of Nck1 and 2 strongly inhibited pathological ocular neovascularization.

We next studied the effect of Nck1 and 2 deletions in the cutaneous wound healing response in adult mice, which is dependent on sprouting angiogenesis. Gene deletion was induced between 6 to 8 weeks of age, the wounds were made at 10 weeks and monitored over the following two weeks (Figure 6E). Wound closure was significantly delayed in *Nck1*$^{-/-}$*Nck2iec* compared with littermate control mice (Figure 6F–G, Supplementary Figure 9).

DISCUSSION

These data provide major insights into how endothelial cells integrate information from multiple environmental cues to control their front-rear polarity during sprouting angiogenesis. They yield the surprising conclusion that VEGF expression and binding to its receptor is not sufficient for front-back polarization and cell migration. Instead, Slit signaling through ROBO receptors is also essential, with NCK1/2 coordinating the functional interaction between the two signaling systems. Furthermore, these effects involve a complex containing ROBO and NCK, which regulates NCK interaction with VEGFR2 and phosphorylation of VEGFR2 on a specific site, Y1214. This pathway then controls activation of Rho GTPases and front-back polarization for endothelial cell migration. The results show that both Vegf-a and Slit2 are required for endothelial cell front-rear polarization and migration, which is mediated by Nck1&2 adaptors that control Cdc42 and Pak2 activation (Figure 7A, B). Nck proteins are known to link extracellular signals to cytoskeletal modifications driving migration in various cell types, but their function in endothelial cells is poorly studied[36–38]. Here we provide the first *in vivo* evidence for their crucial requirement during developmental and pathological angiogenesis, where they promote front-rear endothelial polarity and directional migration.

These data are in agreement with our previous results demonstrating that Slit2/Robo1 function is essential for retinal angiogenesis. Slit2/Robo1 are required to induce Rac1/Pak2 activation and tip cell migration as well as proliferation[19]. Here, we show that Robo1 is also required for VEGF-A induced CDC42 activation and front-rear polarity.

Cdc42, Rac and Pak activation are required for development of front-rear as well as apico-basal polarity[8–11], and also regulate lamellipodia and filopodia formation. It remained unclear how Cdc42 and Rac activation was controlled to mediate the balance between front-rear and apico-basal polarity. Whereas front-rear polarity allows the tip cell to guide the new angiogenic sprout, apico-basal polarity is crucial in the stalk cells to establish a lumen. Polarization and lumen formation are regulated by flow[31, 39] and defects in apico-basal polarity enhance vascular regression and lead to defective anastomosis and remodeling. Our analysis of vascular lumen formation and regression showed no obvious defects in the Nck double mutants, neither at the vascular front, nor in the plexus. Thus, Nck regulation of small Gtpases targets tip cell front-rear polarity, without disturbing apico-basal polarity and endothelial lumen formation in the stalk cells or in the plexus.

Details of the molecular mechanism by which SLIT2-ROBO1&2 and VEGFR2 signaling cooperate through NCK remain to be established. NCK1 can directly bind via its SH3 domain to Proline-rich regions in the ROBO1 cytoplasmic domain[18], and deletion of the PRR domain decreases NCK binding to ROBO1, indicating that ROBO1-NCK interactions in endothelial cells may be direct. NCK can also bind via its SH2 domain to VEGFR2[15, 40], suggesting that NCK1&2 could physically bridge ROBO1 and VEGFR2 following activation by SLIT2 and VEGF. This hypothesis is supported by the absence of VEGF-A induced polarity in the cells transfected with Robo1 lacking the Nck binding domain and by the decrease of Nck/VEGFR2 interactions in cells deleted for ROBO1/2. But this model remains to be proven. These effects may also involve changes in receptor trafficking, which can govern activation and downstream signaling. Regardless of the precise mechanism, *in vivo* and *in vitro* data clearly show that both upstream pathways are crucial for endothelial cell polarized migration and angiogenesis.

The SLIT/ROBO/NCK pathway does not affect VEGFR2 1175, which leads to ERK activation and endothelial cell proliferation[26]. However, SLIT/,ROBO/NCK increases VEGFR2 Y1214 phosphorylation. NCK was reported to bind phosphorylated VEGFR2 Y1214 in HUVEC and to induce downstream CDC42 activation and cell migration[15, 41]. We show that lack of NCK in human and mouse endothelial cells decreases VEGFR2 Y1214 phosphorylation, suggesting existence of additional signalling mediators recruited by NCK that affect this phosphosite. Such signalling mediators could include kinases or phosphatases targeting Y1214. Additional studies are required to identify these mediators, and to elucidate the role of Y1214 in vivo[42]. Our findings show that Notch1 and Alk1 inhibition fails to induce sprouting in the absence of Nck adaptors. Furthermore, pathological ocular neovascularization and wound healing is significantly inhibited in the absence of Slit2/VEGF/NCK-mediated endothelial cell polarization, suggesting that agents that block those targets may have beneficial effects in the treatment of AMD. Slit2 blockade either by soluble Robo1-Fc or inducible genetic deletion of *Slit2* potently inhibits ocular neovascularization without affecting other retinal cells[19]. Together, these studies show that targeting endothelial front-rear polarity via SLIT2, ROBO1/2 and NCK inhibition is a novel approach to prevent vision loss in AMD patients. Unlike current treatments based on pan-VEGF signaling blockade[43, 44], these treatments should spare capillary and photoreceptor survival.

Supplementary Material

Refer to Web version on PubMed Central for supplementary material.

Acknowledgments

We thank Dr Ralf Adams for Cdh5-Cre^{ERT2} mice, Tony Pawson for the *Nck1*−/− and *Nck2*^{lox} mice and Genentech for anti-BMP9 and 10 antibodies.

Funding Sources: This project was supported by grants from NHLBI (1R01HLI125811), NEI (1R01 EY025979-01) and the Agence Nationale de la Recherche (ANR-11BSV102502). A.D and R.O were supported by American Heart Association postdoctoral fellowship awards.

References

1. Herbert SP, Stainier DY. Molecular control of endothelial cell behaviour during blood vessel morphogenesis. Nat Rev Mol Cell Biol. 2011; 12:551–564. [PubMed: 21860391]
2. Potente M, Gerhardt H, Carmeliet P. Basic and therapeutic aspects of angiogenesis. Cell. 2011; 146:873–887. [PubMed: 21925313]
3. Koch S, Claesson-Welsh L. Signal transduction by vascular endothelial growth factor receptors. Cold Spring Harb Perspect Med. 2012; 2:a006502. [PubMed: 22762016]
4. Ferrara N. Vascular endothelial growth factor and age-related macular degeneration: from basic science to therapy. Nat Med. 2010; 16:1107–1111. [PubMed: 20930754]
5. Pavlidis ET, Pavlidis TE. Role of bevacizumab in colorectal cancer growth and its adverse effects: a review. World J Gastroenterol. 2013; 19:5051–5060. [PubMed: 23964138]
6. Stenzel D, Franco CA, Estrach S, Mettouchi A, Sauvaget D, Rosewell I, Schertel A, Armer H, Domogatskaya A, Rodin S, Tryggvason K, Collinson L, Sorokin L, Gerhardt H. Endothelial basement membrane limits tip cell formation by inducing Dll4/Notch signalling in vivo. EMBO Rep. 2011; 12:1135–1143. [PubMed: 21979816]
7. Ricard N, Ciais D, Levet S, Subileau M, Mallet C, Zimmers TA, Lee SJ, Bidart M, Feige JJ, Bailly S. BMP9 and BMP10 are critical for postnatal retinal vascular remodeling. Blood. 2012; 119:6162–6171. [PubMed: 22566602]
8. Etienne-Manneville S, Hall A. Integrin-mediated activation of Cdc42 controls cell polarity in migrating astrocytes through PKCzeta. Cell. 2001; 106:489–498. [PubMed: 11525734]
9. Etienne-Manneville S, Hall A. Rho GTPases in cell biology. Nature. 2002; 420:629–635. [PubMed: 12478284]
10. Etienne-Manneville S, Hall A. Cdc42 regulates GSK-3beta and adenomatous polyposis coli to control cell polarity. Nature. 2003; 421:753–756. [PubMed: 12610628]
11. Fukata M, Nakagawa M, Kaibuchi K. Roles of Rho-family GTPases in cell polarisation and directional migration. Curr Opin Cell Biol. 2003; 15:590–597. [PubMed: 14519394]
12. Li W, Fan J, Woodley DT. Nck/Dock: an adapter between cell surface receptors and the actin cytoskeleton. Oncogene. 2001; 20:6403–6417. [PubMed: 11607841]
13. Buday L, Wunderlich L, Tamas P. The Nck family of adapter proteins: regulators of actin cytoskeleton. Cell Signal. 2002; 14:723–731. [PubMed: 12034353]
14. Bladt F, Aippersbach E, Gelkop S, Strasser GA, Nash P, Tafuri A, Gertler FB, Pawson T. The murine Nck SH2/SH3 adaptors are important for the development of mesoderm-derived embryonic structures and for regulating the cellular actin network. Mol Cell Biol. 2003; 23:4586–4597. [PubMed: 12808099]
15. Lamalice L, Houle F, Huot J. Phosphorylation of Tyr1214 within VEGFR-2 triggers the recruitment of Nck and activation of Fyn leading to SAPK2/p38 activation and endothelial cell migration in response to VEGF. J Biol Chem. 2006; 281:34009–34020. [PubMed: 16966330]
16. Fan X, Labrador JP, Hing H, Bashaw GJ. Slit stimulation recruits Dock and Pak to the roundabout receptor and increases Rac activity to regulate axon repulsion at the CNS midline. Neuron. 2003; 40:113–127. [PubMed: 14527437]

17. Ballard MS, Hinck L. A roundabout way to cancer. Adv Cancer Res. 2012; 114:187–235. [PubMed: 22588058]
18. Fan X, Li Q, Pisarek-Horowitz A, Rasouly HM, Wang X, Bonegio RG, Wang H, McLaughlin M, Mangos S, Kalluri R, Holzman LB, Drummond IA, Brown D, Salant DJ, Lu W. Inhibitory effects of Robo2 on nephrin: a crosstalk between positive and negative signals regulating podocyte structure. Cell Rep. 2012; 2:52–61. [PubMed: 22840396]
19. Rama N, Dubrac A, Mathivet T, Ni Charthaigh RA, Genet G, Cristofaro B, Pibouin-Fragner L, Ma L, Eichmann A, Chedotal A. Slit2 signaling through Robo1 and Robo2 is required for retinal neovascularization. Nat Med. 2015; 21:483–491. [PubMed: 25894826]
20. Simons M, Alitalo K, Annex BH, Augustin HG, Beam C, Berk BC, Byzova T, Carmeliet P, Chilian W, Cooke JP, Davis GE, Eichmann A, Iruela-Arispe ML, Keshet E, Sinusas AJ, Ruhrberg C, Woo YJ, Dimmeler S. American Heart Association Council on Basic Cardiovascular S, Council on Cardiovascular S and Anesthesia. State-of-the-Art Methods for Evaluation of Angiogenesis and Tissue Vascularization: A Scientific Statement From the American Heart Association. Circ Res. 2015; 116:e99–e132. [PubMed: 25931450]
21. Clouthier DL, Harris CN, Harris RA, Martin CE, Puri MC, Jones N. Requisite role for Nck adaptors in cardiovascular development, endothelial-to-mesenchymal transition, and directed cell migration. Mol Cell Biol. 2015; 35:1573–1587. [PubMed: 25691664]
22. Fawcett JP, Georgiou J, Ruston J, Bladt F, Sherman A, Warner N, Saab BJ, Scott R, Roder JC, Pawson T. Nck adaptor proteins control the organization of neuronal circuits important for walking. Proc Natl Acad Sci U S A. 2007; 104:20973–20978. [PubMed: 18093944]
23. Jones N, Blasutig IM, Eremina V, Ruston JM, Bladt F, Li H, Huang H, Larose L, Li SS, Takano T, Quaggin SE, Pawson T. Nck adaptor proteins link nephrin to the actin cytoskeleton of kidney podocytes. Nature. 2006; 440:818–823. [PubMed: 16525419]
24. Wang Y, Nakayama M, Pitulescu ME, Schmidt TS, Bochenek ML, Sakakibara A, Adams S, Davy A, Deutsch U, Luthi U, Barberis A, Benjamin LE, Makinen T, Nobes CD, Adams RH. Ephrin-B2 controls VEGF-induced angiogenesis and lymphangiogenesis. Nature. 2010; 465:483–486. [PubMed: 20445537]
25. Birdsey GM, Dryden NH, Amsellem V, Gebhardt F, Sahnan K, Haskard DO, Dejana E, Mason JC, Randi AM. Transcription factor Erg regulates angiogenesis and endothelial apoptosis through VE-cadherin. Blood. 2008; 111:3498–3506. [PubMed: 18195090]
26. Eichmann A, Simons M. VEGF signaling inside vascular endothelial cells and beyond. Curr Opin Cell Biol. 2012; 24:188–193. [PubMed: 22366328]
27. Larrivee B, Prahst C, Gordon E, del Toro R, Mathivet T, Duarte A, Simons M, Eichmann A. ALK1 signaling inhibits angiogenesis by cooperating with the Notch pathway. Dev Cell. 2012; 22:489–500. [PubMed: 22421041]
28. del Toro R, Prahst C, Mathivet T, Siegfried G, Kaminker JS, Larrivee B, Breant C, Duarte A, Takakura N, Fukamizu A, Penninger J, Eichmann A. Identification and functional analysis of endothelial tip cell-enriched genes. Blood. 2010; 116:4025–4033. [PubMed: 20705756]
29. Zovein AC, Luque A, Turlo KA, Hofmann JJ, Yee KM, Becker MS, Fassler R, Mellman I, Lane TF, Iruela-Arispe ML. Beta1 integrin establishes endothelial cell polarity and arteriolar lumen formation via a Par3-dependent mechanism. Dev Cell. 2010; 18:39–51. [PubMed: 20152176]
30. Xu K, Sacharidou A, Fu S, Chong DC, Skaug B, Chen ZJ, Davis GE, Cleaver O. Blood vessel tubulogenesis requires Rasip1 regulation of GTPase signaling. Dev Cell. 2011; 20:526–539. [PubMed: 21396893]
31. Phng LK, Gebala V, Bentley K, Philippides A, Wacker A, Mathivet T, Sauteur L, Stanchi F, Belting HG, Affolter M, Gerhardt H. Formin-mediated actin polymerization at endothelial junctions is required for vessel lumen formation and stabilization. Dev Cell. 2015; 32:123–132. [PubMed: 25584798]
32. Wang B, Xiao Y, Ding BB, Zhang N, Yuan X, Gui L, Qian KX, Duan S, Chen Z, Rao Y, Geng JG. Induction of tumor angiogenesis by Slit-Robo signaling and inhibition of cancer growth by blocking Robo activity. Cancer Cell. 2003; 4:19–29. [PubMed: 12892710]
33. Geudens I, Gerhardt H. Coordinating cell behaviour during blood vessel formation. Development. 2011; 138:4569–4583. [PubMed: 21965610]

34. David L, Mallet C, Keramidas M, Lamande N, Gasc JM, Dupuis-Girod S, Plauchu H, Feige JJ, Bailly S. Bone morphogenetic protein-9 is a circulating vascular quiescence factor. Circ Res. 2008; 102:914–922. [PubMed: 18309101]

35. David L, Mallet C, Mazerbourg S, Feige JJ, Bailly S. Identification of BMP9 and BMP10 as functional activators of the orphan activin receptor-like kinase 1 (ALK1) in endothelial cells. Blood. 2007; 109:1953–1961. [PubMed: 17068149]

36. Chaki SP, Barhoumi R, Berginski ME, Sreenivasappa H, Trache A, Gomez SM, Rivera GM. Nck enables directional cell migration through the coordination of polarized membrane protrusion with adhesion dynamics. J Cell Sci. 2013; 126:1637–1649. [PubMed: 23444376]

37. Chaki SP, Rivera GM. Integration of signaling and cytoskeletal remodeling by Nck in directional cell migration. Bioarchitecture. 2013; 3:57–63. [PubMed: 23887203]

38. Chaki SP, Barhoumi R, Rivera GM. Actin remodeling by Nck regulates endothelial lumen formation. Mol Biol Cell. 2015; 26:3047–3060. [PubMed: 26157164]

39. Franco CA, Jones ML, Bernabeu MO, Geudens I, Mathivet T, Rosa A, Lopes FM, Lima AP, Ragab A, Collins RT, Phng LK, Coveney PV, Gerhardt H. Dynamic endothelial cell rearrangements drive developmental vessel regression. PLoS Biol. 2015; 13:e1002125. [PubMed: 25884288]

40. Kroll J, Waltenberger J. The vascular endothelial growth factor receptor KDR activates multiple signal transduction pathways in porcine aortic endothelial cells. J Biol Chem. 1997; 272:32521–32527. [PubMed: 9405464]

41. Lamalice L, Houle F, Jourdan G, Huot J. Phosphorylation of tyrosine 1214 on VEGFR2 is required for VEGF-induced activation of Cdc42 upstream of SAPK2/p38. Oncogene. 2004; 23:434–445. [PubMed: 14724572]

42. Sakurai Y, Ohgimoto K, Kataoka Y, Yoshida N, Shibuya M. Essential role of Flk-1 (VEGF receptor 2) tyrosine residue 1173 in vasculogenesis in mice. Proc Natl Acad Sci U S A. 2005; 102:1076–1081. [PubMed: 15644447]

43. Kurihara T, Westenskow PD, Bravo S, Aguilar E, Friedlander M. Targeted deletion of Vegfa in adult mice induces vision loss. J Clin Invest. 2012; 122:4213–4217. [PubMed: 23093773]

44. Nishijima K, Ng YS, Zhong L, Bradley J, Schubert W, Jo N, Akita J, Samuelsson SJ, Robinson GS, Adamis AP, Shima DT. Vascular endothelial growth factor-A is a survival factor for retinal neurons and a critical neuroprotectant during the adaptive response to ischemic injury. Am J Pathol. 2007; 171:53–67. [PubMed: 17591953]

Clinical Perspectives

Sprouting angiogenesis drives neovascularization in pathologies including age-related macular degeneration, wound healing, and cancer. Endothelial cells forming the sprout switch from a lumenized phenotype with apico-basal polarity to a non-lumenized tip cell with front-rear polarity. Here we show that the Nck1 and 2 adaptor proteins are required for endothelial cell front-rear polarity and sprouting angiogenesis. Mice carrying inducible, endothelialspecific Nck1/2 deletions fail to develop front-rear polarized vessel sprouts and exhibit severe sprouting angiogenesis defects. Mechanistically, NCK1 and 2 promote polarity by activating Cdc42 and Pak2 downstream of VEGF-A and Slit2 signaling pathways. NCK1/2 coordinates the functional interaction between VEGF-A and Slit2 signaling required for front-rear polarity and sprouting angiogenesis. Targeting this interaction inhibits pathological ocular angiogenesis and wound healing, allowing for generation of novel therapeutics to prevent neovascularization.

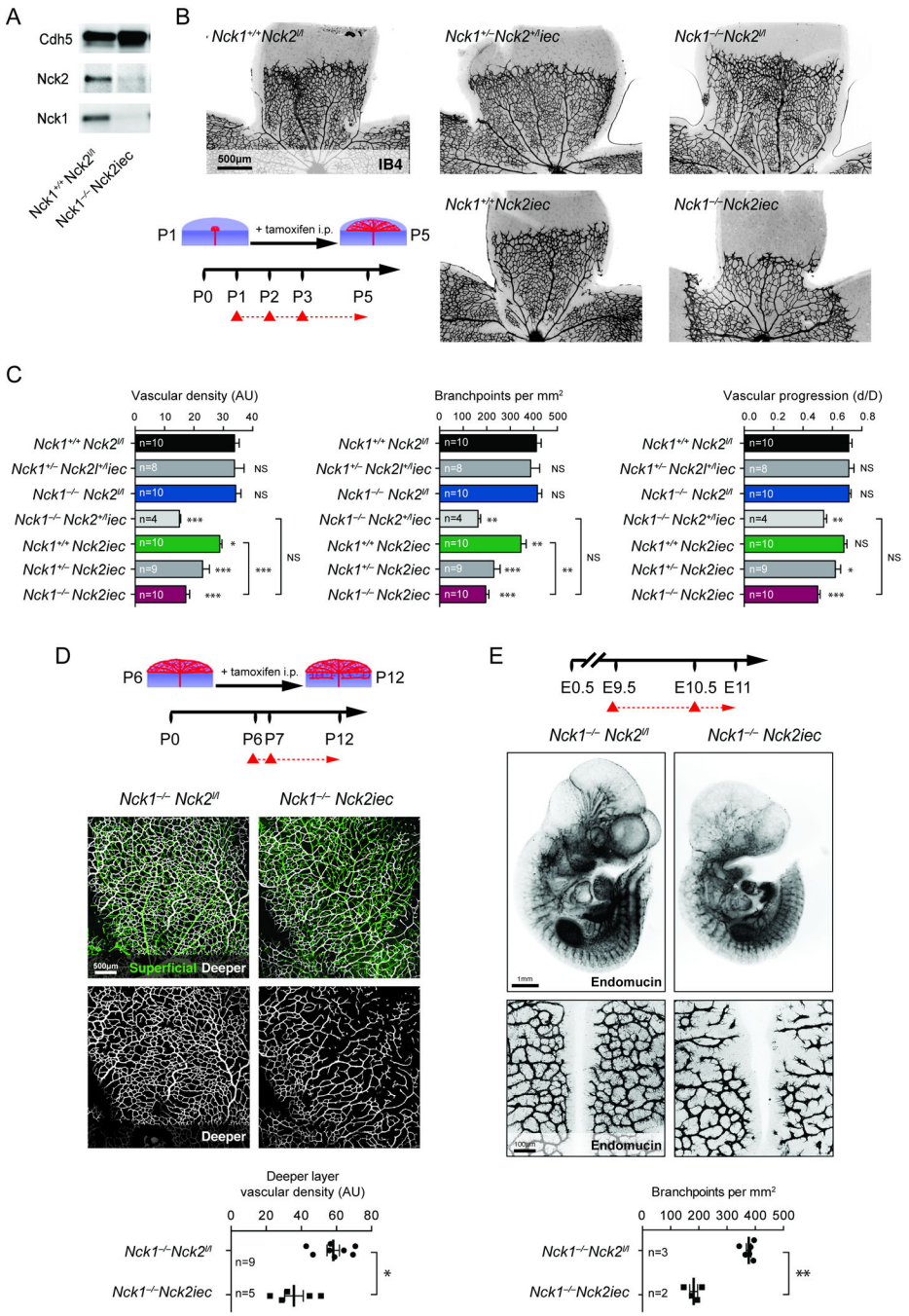

Figure 1.

Endothelial Nck adaptors are required for retinal angiogenesis. **A,** Western-blot against Nck1, Nck2 and VE-cadherin on P12 purified mouse lung endothelial cells (MLEC) isolated from P1/2/3 tamoxifen injected mice. **B,** Left bottom, schematic of the experimental strategy to assess early formation of the retinal vasculature (P1-P5). The red triangles indicate the intraperitoneal injections of tamoxifen at P1/2/3. Retinal flat mounts of P5 mice with the indicated genotypes are stained with IB4 (negative images of the fluorescent signal). **C,** Quantification of vascular density, number of branchpoints and vascular progression.

Number of retinas used for quantification is indicated (*p*-values are versus *Nck1*$^{+/+}$*Nck2*$^{l/l}$). **D,** Top, schematic of the experimental strategy to assess late development of the retinal vasculature (P6-P12) in *Nck1*$^{-/-}$*Nck2iec* mice. Middle, Retinal flat mounts of P12 mice stained with IB4, the superficial vascular layer is represented in green and the deeper vascular layer in white. Bottom, quantification of the vascular density of the deeper layer. Number of retinas used for quantification is indicated. **E,** Top panel, schematic of the experimental strategy. Middle, whole mount Endomucin staining of E11 embryos (n=5 embryos for *Nck1*$^{-/-}$*Nck2*$^{l/l}$ and n=3 embryos for *Nck1*$^{+/+}$*Nck2iec*). Bottom, flatmounts of hindbrain vascular plexus and branchpoint quantification per mm^2. Number of hindbrains used for quantification is indicated. Results are presented as mean ± s.e.m and statistical significance was analyzed by Mann-Whitney *U* test. *P<0.05, **P<0.01, ***P<0.001, NS: non significant.

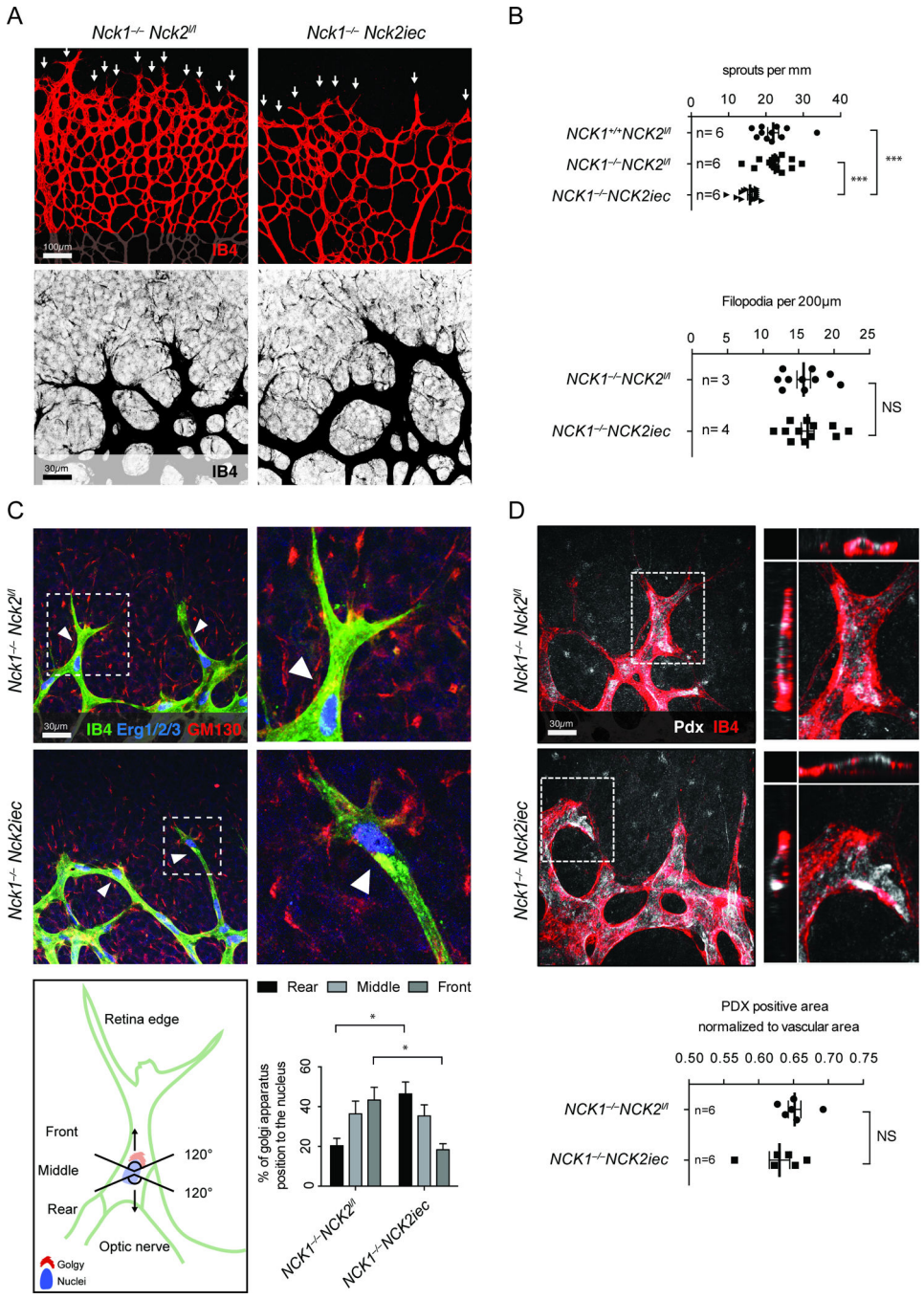

Figure 2.

Nck regulates tip cell front-rear polarization. **A,** Top, sprouting front of P5 retina stained with IB4, the sprouting tip cells are indicated with arrows. Bottom, higher magnification of filopodial extensions. **B,** Quantification of sprouts and filopodia numbers at the angiogenic front. Number of retinas used for quantification is indicated. **C,** Top left**,** IsoB4 (green), Gm130 (red) and Erg1/2/3 (blue) triple-labeling shows Golgi polarization (arrowheads) of P5 tip cells. Top right panels are higher magnifications. Bottom left, Golgi orientation of the tip cell during sprouting angiogenesis. Bottom right, quantification of the Golgi positions

(n=4 retina for *Nck1*$^{-/-}$*Nck2*$^{l/l}$ and n=4 retina for *Nck1*$^{+/+}$*Nck2iec*, at least 50 tip cells per retina were quantified). **D,** Top left, IB4 (red) and podocalyxin (Pdx, white) staining of P5 retinas. Top right, 3D view of tip cell with orthogonal slices, xz (left) and yz (top) planes. Bottom, quantification of Pdx staining. Number of retinas used for quantification is indicated. Results are presented as mean ± s.e.m and statistical significance was analyzed by Mann-Whitney *U* test. *P<0.05, **P<0.01, ***P<0.001, NS: non significant.

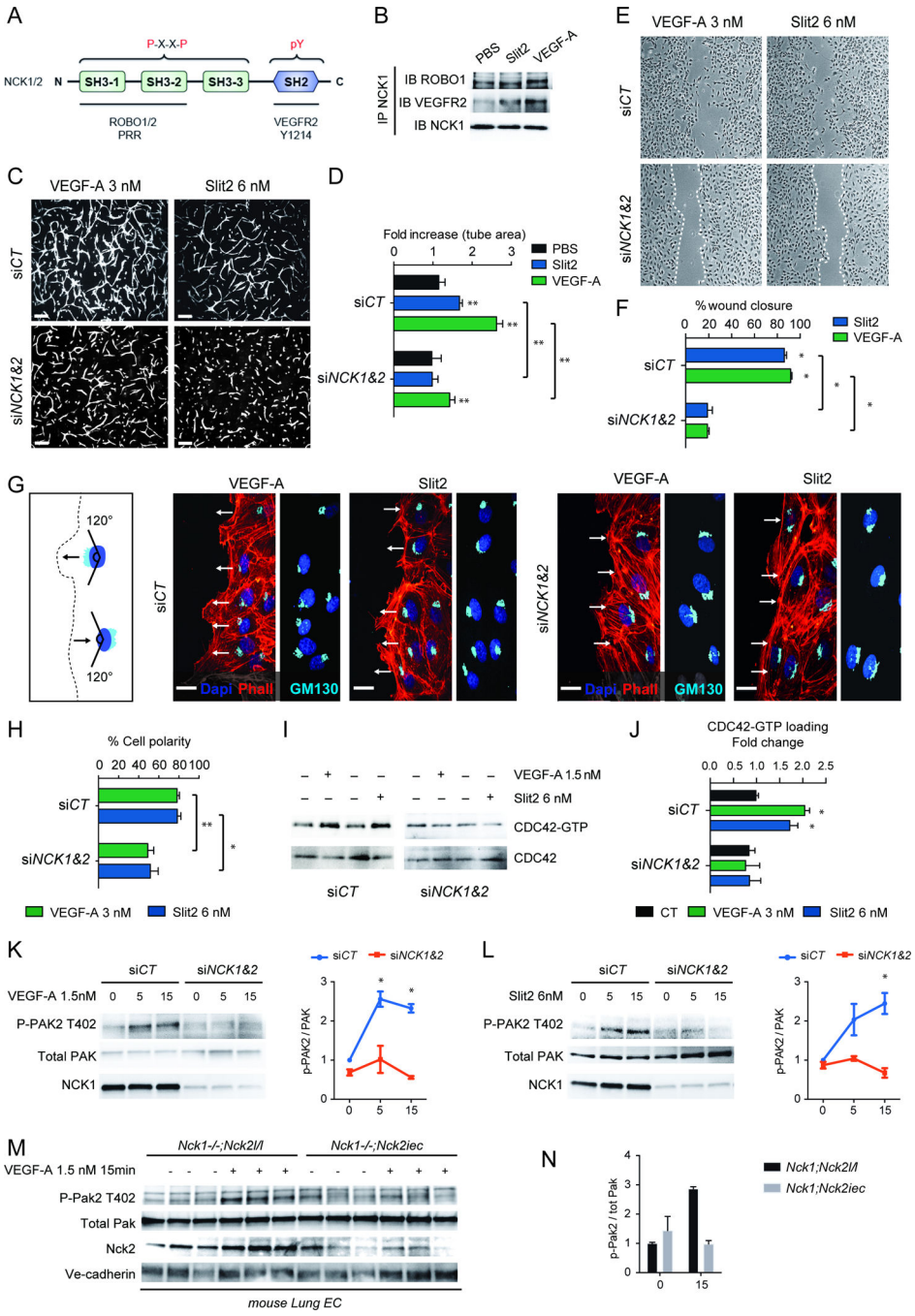

Figure 3.

NCK is required for polarized endothelial cell migration. **A,** Structural domains of NCK1 and 2 indicating VEGFR2 and ROBO1 binding domains and the consensus sequence found in proteins that bind NCK. **B,** Co-immunoprecipitation of ROBO1 and VEGFR2 with NCK1. Cells were treated with PBS, Slit2 (6 nM) or VEGF (3 nM) for 5min followed by NCK1 IP and immunoblot with anti-ROBO1 or anti-VEGFR2 antibodies. **C,** Combined *NCK1/2* knockdown decreases VEGF-A and Slit2-induced sprouting in 3D-fibrin gels. **D,** Quantification of sprouting (n= 6). Results are presented as mean ± s.e.m., statistical

analyses were performed using Mann-Whitney *U* test. *P<0.05, **P<0.01. **E,** *NCK1/2* knockdown decreases VEGF-A and Slit2-induced scratch wound migration after 24h. **F,** Quantification of wound closure (n= 4). Results are presented as mean ± s.e.m., statistical analyses were performed using Mann-Whitney *U* test. *P<0.05. **G,** Golgi orientation during migration. Phalloidin (red) DAPI (blue) staining combined with Golgi labeling by GM130 (light blue) in HUVECs at the scratch wound edge (left) 2h after wounding. Golgi polarization in front of the nucleus (arrows indicate direction of migration) is impaired in *NCK1/2* knockdown cells. **H,** Quantification of the % of cells polarized (n=4, 120–150 cells were analyzed in each individual experiments). Results are presented as mean ± s.e.m., statistical analyses were performed using Student's t-test. *P<0.05, **P<0.01. **I,** *NCK1/2* siRNA inhibits CDC42-GTP loading induced by VEGF-A and Slit2 (5min stimulation). **J,** Quantification (n=5). Results are presented as mean ± s.e.m., statistical analyses were performed using Mann-Whitney *U* test. *P<0.05. **K, L,** Western-blot analysis and quantification of VEGF-A or Slit2 induced PAK2 activation (n=3) in HUVECs with *NCK1/2* siRNA transfection. Results are presented as mean ± s.e.m., statistical analyses were performed using Kruskal-Wallis test with Dunn's multiple comparisons test. *P<0.05. **M,** Western-blot against Phospho-Pak2 using MLEC from 3 different $Nck1^{-/-}Nck2^{l/l}$ or $Nck1^{-/-}$*Nck2iec* mice stimulated with VEGF-A during 15min. **N,** Quantification.

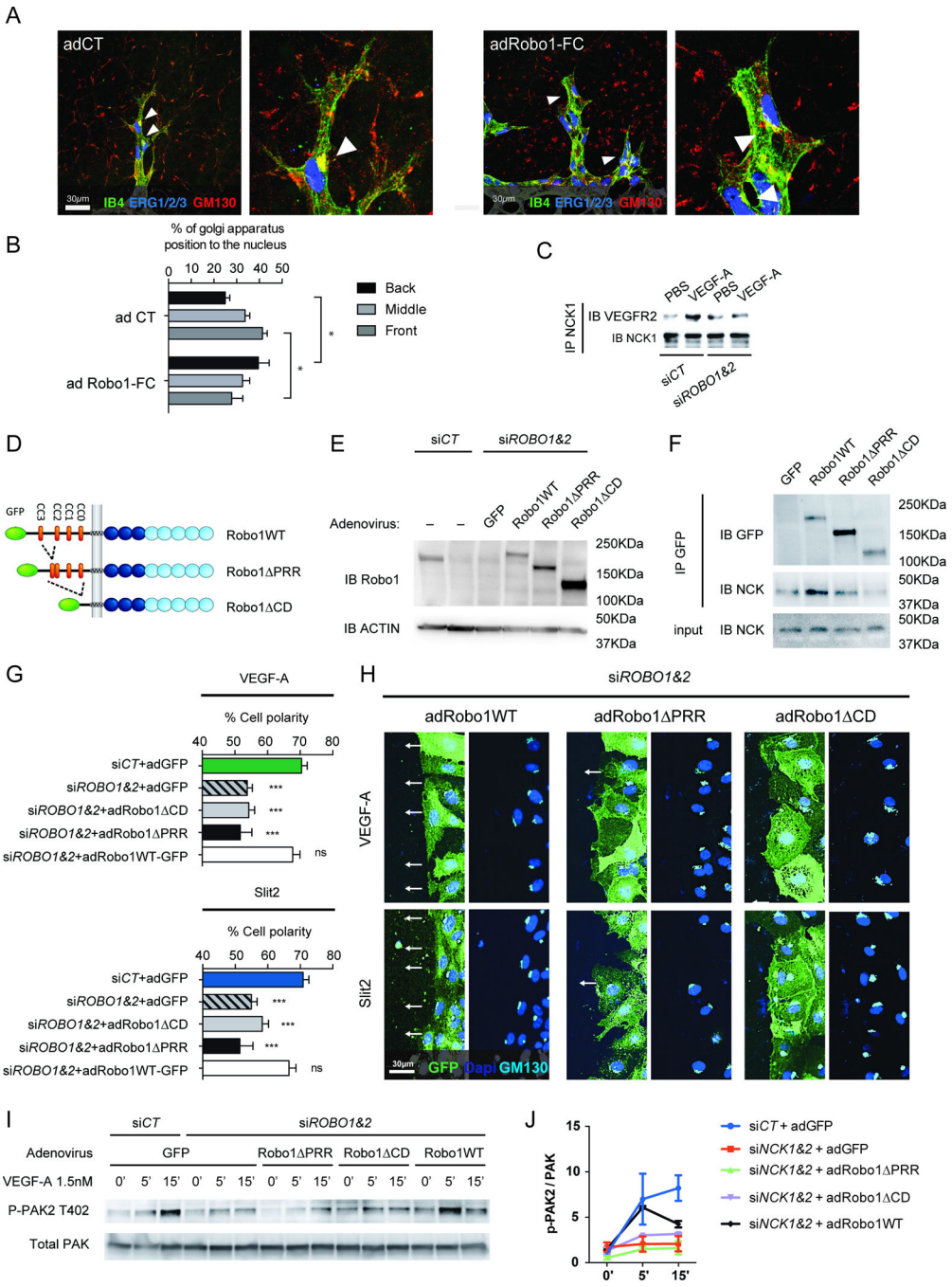

Figure 4.

Slit2/ROBO1/NCK are required for VEGF-A induced front-rear polarity. **A,** Retinal IB4 (green), Gm130 (red) and Erg1/2/3 (blue) triple-labeling of mice injected with control or Robo1-Fc adenovirus. **B,** Quantification of the different Golgi positions around the nuclei toward the migrating front (n=3 retina for *Nck1*$^{-/-}$*Nck2*$^{l/l}$ and n=3 retina for *Nck1*$^{+/+}$*Nck2iec*, at least 50 tip cells per retina were quantified). Results are presented as mean ± s.e.m., statistical analyses were performed using Mann-Whitney *U* test. *P<0.05. **C,** *ROBO1/2* siRNA reduces co-IP between NCK1 and VEGFR2 following VEGF stimulation. **D,**

Schematic diagram of CD-truncated Robo1 mutants. **E,** Western-blot of Robo1WT-GFP and mutants in *ROBO1/2* siRNA transfected HUVECs. **F,** Co-immunoprecipitation of Robo1WT-GFP and mutants with NCK1. **G, H,** Golgi orientation of *ROBO1/2* deleted HUVEC expressing the different Robo1 variants (n=3). **I, J,** Western-blot analysis and quantification of VEGF-A induced PAK2 activation (n=2) in HUVECs with *ROBO1/2* siRNA transfection and adenovirus infection. Results are presented as mean ± s.e.m., statistical analyses were performed using Student's t-test. *P<0.05, **P<0.01, ***P<0.001, NS: non significant.

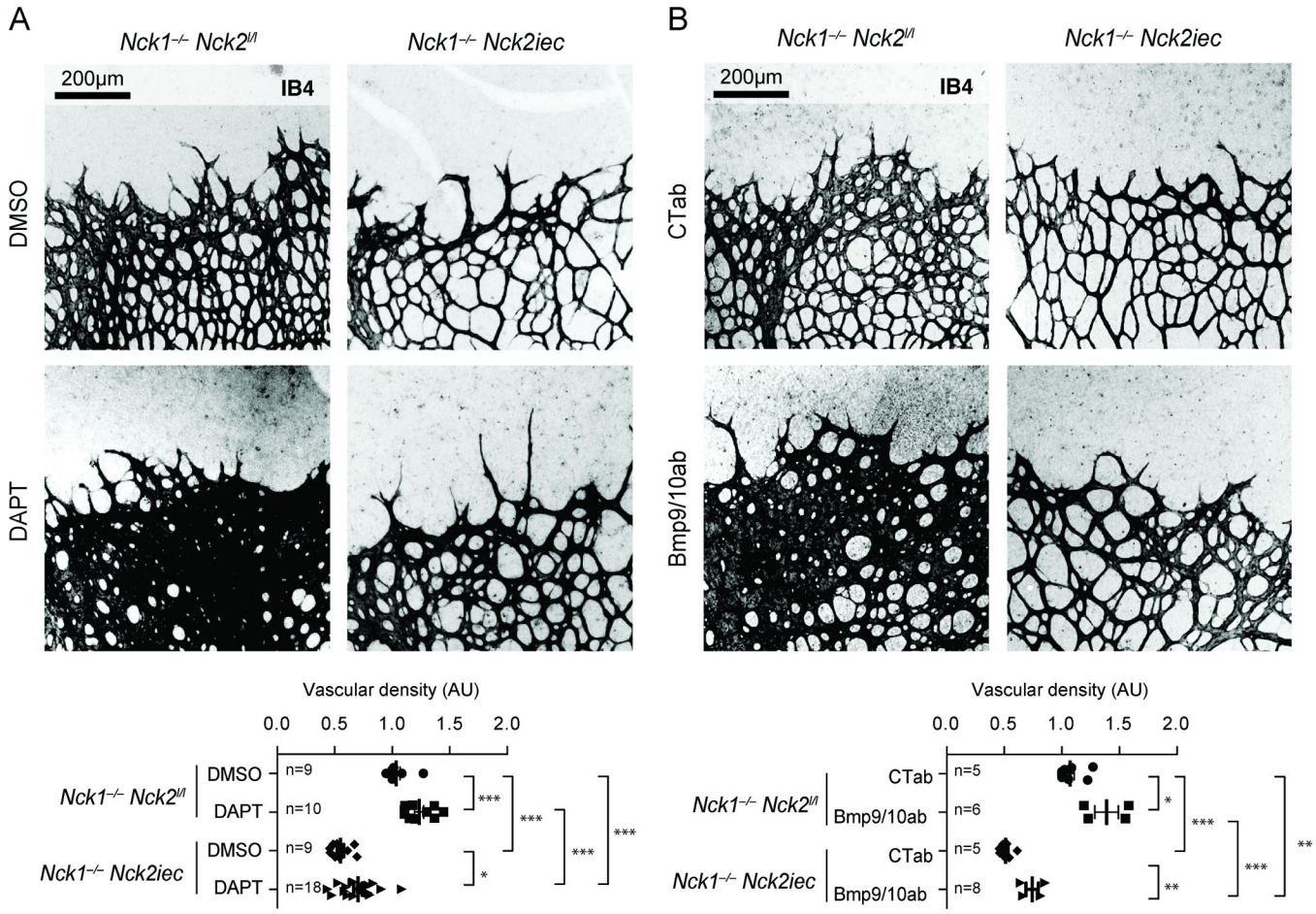

Figure 5.

Nck deletion prevents hypersprouting induced by Notch and Alk1 inhibition. **A,** DAPT induced hypersprouting in *Nck1/2* mutant retinas. Bottom panel, quantification of the vascular density. Number of retinas used for quantification is indicated. **B,** Bmp9 and 10 blocking antibodies induced hypersprouting in *Nck1/2* mutant retinas. Bottom panel, quantification of the vascular density. Number of retinas used for quantification is indicated. Results are presented as mean ± s.e.m and statistical significance was analyzed by Mann-Whitney *U* test. *P<0.05, **P<0.01, ***P<0.001.

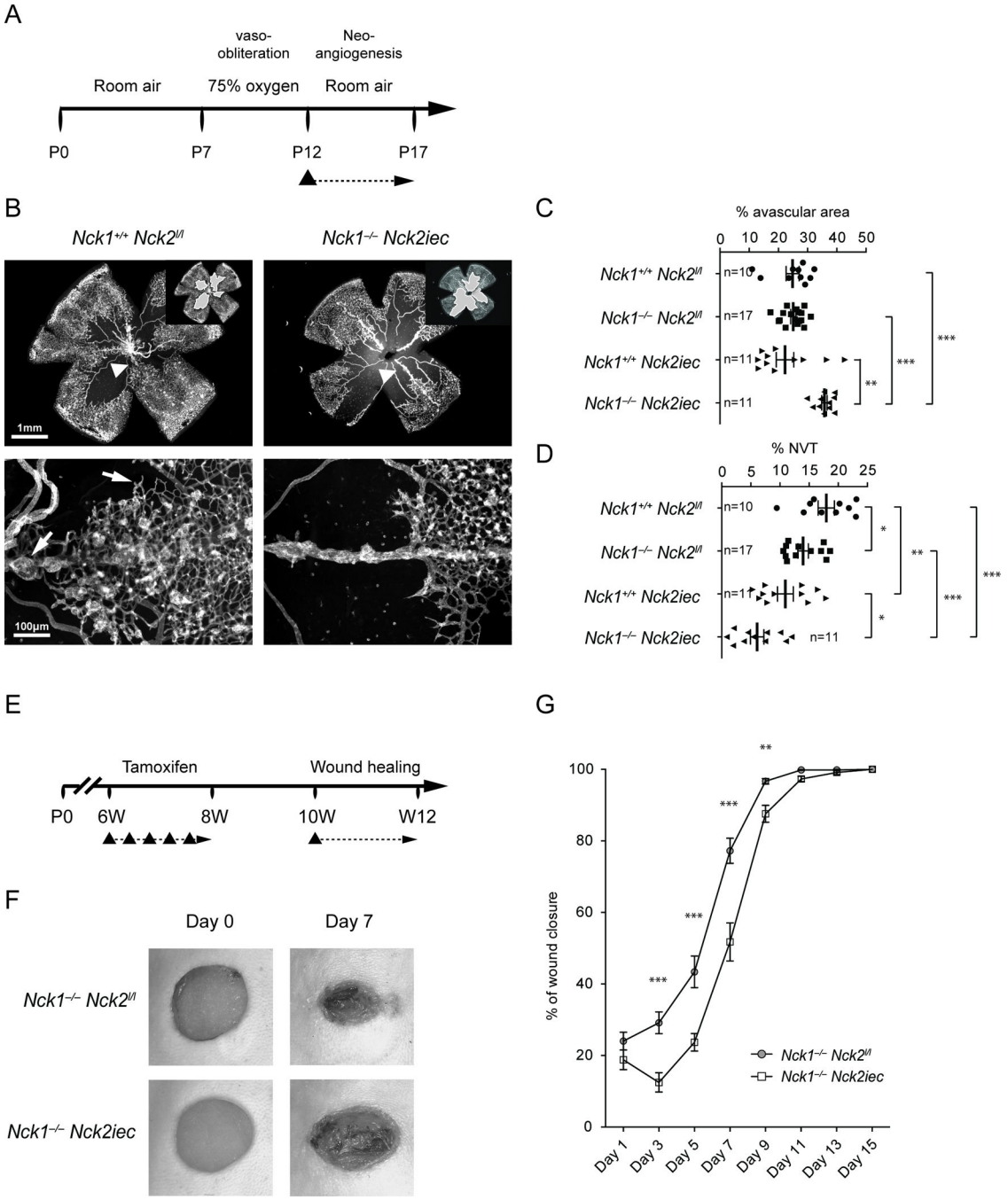

Figure 6.

Endothelial Ncks are required for pathological angiogenesis. **A,** Schematic of the experimental strategy to assess neo-angiogenesis after oxygen-induced retinopathy (OIR). The triangle indicates the intraperitoneal injection of tamoxifen at P12. **B,** Retinal flat mounts after OIR. Insets show avascular area measured for quantification. Lower panels show higher magnification images of pathological vascular tufts. Note reduction of sprouting and tuft formation in *Nck1*$^{-/-}$*Nck2iec* double mutants mice. **C, D,** Avascular area (c) and neovascular tuft (d) quantification. Number of retinas used for quantification is

indicated. Graphs represent mean±SEM and statistical significance was assessed using a Mann-Whitney *U* test. *P<0.05, **P<0.01, ***P<0.001. NVT: neo-vascular tuft. **E,** Schematic of the experimental strategy to assess wound healing after *Nck1* and *2* deletions. The triangle indicates the intraperitoneal injection of tamoxifen at 6 weeks of age and the skin wound at 10 weeks of age. **F**, Representative images of wound healing in *Nck1*$^{-/-}$*Nck2iec* and control littermate mice after wounding by punch biopsy. **G**, Quantification of wound closure area (n=14, *Nck1*$^{-/-}$*Nck2*$^{l/l}$ and n=14 *Nck1*$^{-/-}$*Nck2iec* mice). Graphs represent mean±SEM and statistical significance was assessed using a Mann-Whitney *U* test. **P<0.01, ***P<0.001.

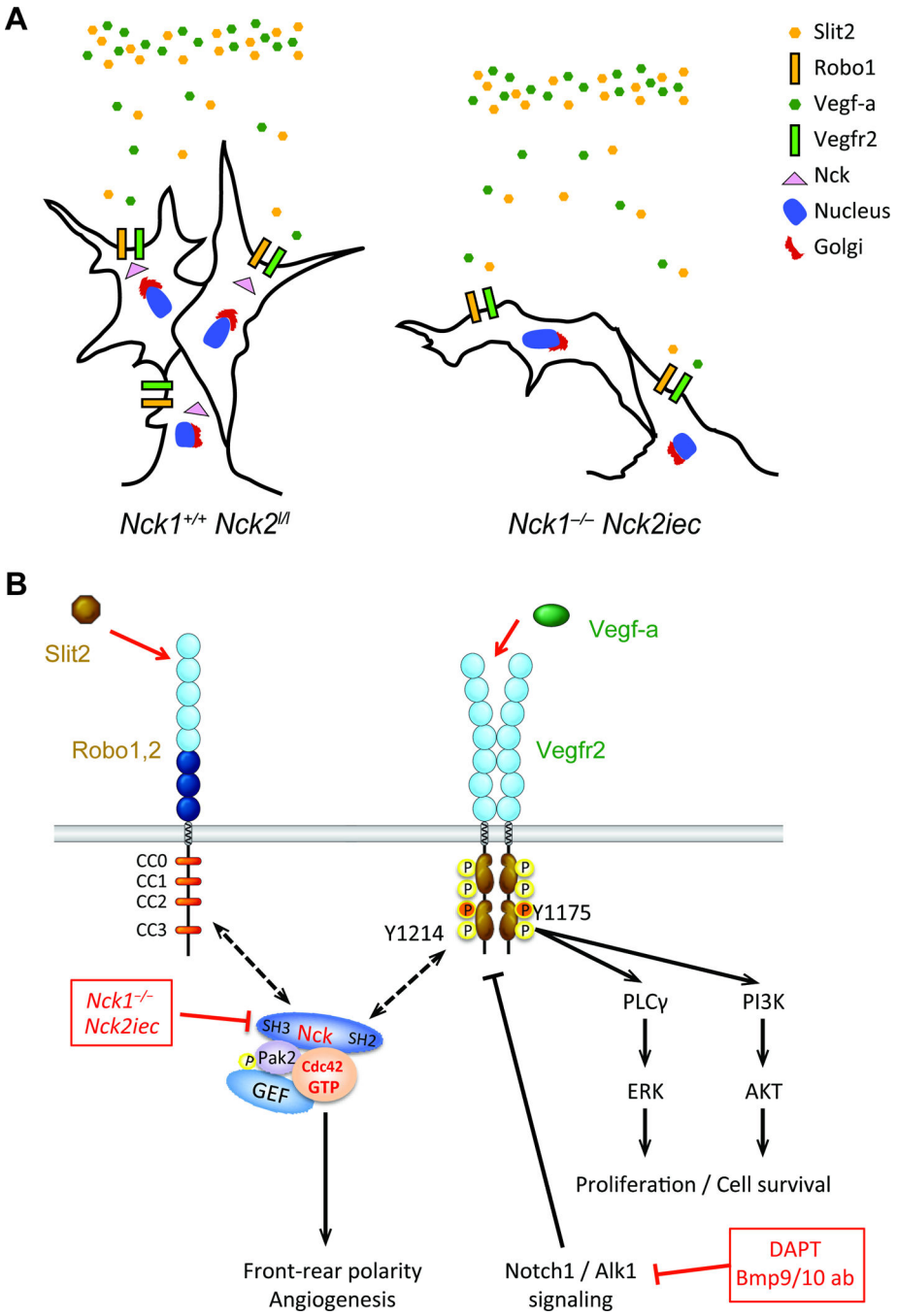

Figure 7.

Model for endothelial Nck1 and 2 function. **A,** Proposed model for the tip cell migration defect observed in *Nck1,2* knockout mice. Nck1 and 2 selectively regulate VEGF-A and Slit2 induced tip cell front-rear polarity. **B,** Proposed model for regulation of cell polarity and CDC42 activation downstream of VEGFR2 and ROBO1.